© 2014. Published by The Company of Biologists Ltd | Journal of Cell Science (2014) 127, 465–474 doi:10.1242/jcs.142737

RESEARCH ARTICLE

Specification of leading and trailing cell features during collective migration in the *Drosophila* trachea

Gaëlle Lebreton[1,2,*] and Jordi Casanova[1,2,*]

ABSTRACT

The role of tip and rear cells in collective migration is still a matter of debate and their differences at the cytoskeletal level are poorly understood. Here, we analysed these issues in the *Drosophila* trachea, an organ that develops from the collective migration of clusters of cells that respond to Branchless (Bnl), a fibroblast growth factor (FGF) homologue expressed in surrounding tissues. We track individual cells in the migratory cluster and characterise their features and unveil two prototypical types of cytoskeletal organisation that account for tip and rear cells respectively. Indeed, once the former are specified, they remain as such throughout migration. Furthermore, we show that FGF signalling in a single tip cell can trigger the migration of the cells in the branch. Finally, we found specific Rac activation at the tip cells and analysed how FGF-independent cell features, such as adhesion and motility, act on coupling the behaviour of trailing and tip cells. Thus, the combined effect of FGF promoting leading cell behaviour and the modulation of cell properties in a cluster can account for the wide range of migratory events driven by FGF.

KEY WORDS: *Drosophila*, Migration, Branchless, FGF

INTRODUCTION

Collective cell migration is a widespread phenomenon in many biological processes, both in development and in disease conditions. Distinct cell types have been identified in migrating clusters, which have been suggested to display different cell activity, namely leading cells at the tip front and trailing cells at the rear. However, the role of tip and rear cells in collective migration is still a matter of debate (Rørth, 2012). Moreover, what makes these cells behave distinctly and their differences at the cytoskeletal level are poorly understood (Friedl and Gilmour, 2009; Rørth, 2012).

The tracheal system of *Drosophila* is a particularly tractable model for the study of cell migration, and, in particular, of the mechanisms that guide cells to migrate in specific directions (Ghabrial et al., 2003). The *Drosophila* tracheal system develops from two clusters of cells in the ectoderm, one at each side of the central body segments. These cells invaginate, forming the tracheal pits (Ghabrial et al., 2003). The cells of each cluster invaginate and migrate in different and stereotyped directions (Samakovlis et al., 1996) by responding to Branchless (Bnl), a fibroblast growth factor (FGF) homologue expressed around the developing tracheal system in cells at each position in which a new branch will form and grow. Activation of the Breathless (Btl) receptor in the tracheal cells by Bnl is thought to stimulate and guide tracheal migration towards these positions (Sutherland et al., 1996). Tracheal cell division stops just as primary branching begins and there is no fixed lineage relationship among cells contributing to a given branch or sharing the same position or fate in a branch (Samakovlis et al., 1996). Interestingly, FGF is also required for cell migration in other morphogenetic events, such as in the development of the zebrafish lateral line (Aman and Piotrowski, 2008; Lecaudey et al., 2008), and in gastrulation in both invertebrates and vertebrates (Griffin et al., 1995; Ciruna and Rossant, 2001; for a review, see Bae et al., 2012). However, in spite of the wide use of the *Drosophila* tracheal system as a model for FGF-triggered migration, it is not known what the role, specification and cytological features of tip and rear cell cells are and which cells require FGF signalling to sustain collective migration. In this work, we have investigated these issues by the analysis of a particular branch from the developing tracheal cell cluster.

[1]Institut de Biologia Molecular de Barcelona (CSIC), C/Baldiri Reixac 4–8, 08028 Barcelona, Spain. [2]Institut de Recerca Biomèdica de Barcelona, C/Baldiri Reixac 10, 08028 Barcelona, Spain.

*Authors for correspondence (jcrbmc@ibmb.csic.es; gaellb@gmail.com)

Received 16 September 2013; Accepted 24 October 2013

RESULTS

Morphological features of leading and trailing and cells in the lateral trunk posterior and ganglionic branch

Among the tracheal branches from each placode, two grow towards the ventral side of the embryo, one in the anterior and the other in the posterior region of the segment, the lateral trunk anterior (LTa) and the lateral trunk posterior (LTp), respectively (Fig. 1A–E). By a combination of migration, intercalation and elongation, the tip cell of the LTp migrates towards the central nervous system (CNS), and the resulting ganglionic branch (GB) connects the CNS to the main tracheal tube (Fig. 1E, red arrowheads). Another cell from the LTp migrates towards the LTa of the adjacent posterior metamere and makes a fusion branch that connects the two LT branches (Fig. 1D,E, red arrows) (Ghabrial et al., 2003). We decided to focus on this branch (LTp/GB) because its complex morphology and pattern of migration make it particularly appropriate for analysing the morphology and behaviour of the tip and trailing cell during tracheal collective migration.

Live recording and individual cell labelling have completely changed our view of how cells migrate collectively (Rørth, 2012), and have hence become an essential part of morphogenesis studies. Individual cell labelling showed that tracheal cells upon invagination were rounded basally and constricted on the apical side, which faces the inner cavity of the tracheal pit (Fig. 1F, Fig. 2A). Subsequently, these cells, while keeping their constricted apical surface, had an elongated body and became bottle-shaped (Fig. 1G, Fig. 2B). By early stage 12, the small bud that will give rise to the LTp/GB branch was identifiable

Journal of Cell Science (2014) 127, 465–474 doi:10.1242/jcs.142737

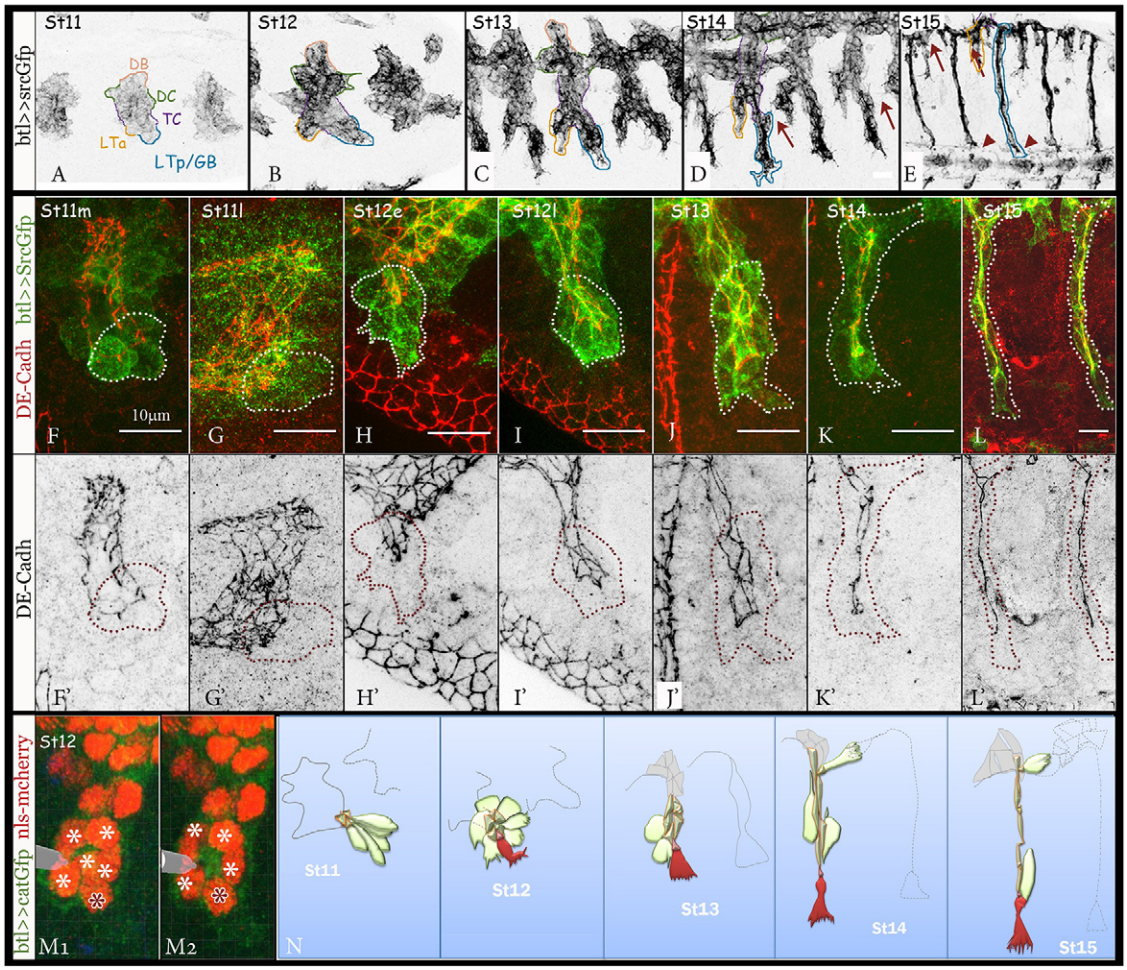

Fig. 1. Development of the LTp/GB. (A–E) Overview of tracheal development with a focus on LTp/GBs (highlighted in blue). Red arrows, cells forming the LTp; red arrowheads, tip cell of the GB reaching the CNS. (F–L) LTp/GB morphogenesis at budding (F–H), elongation (I–L) and intercalation (K,L). (F′–L′) Same panels showing DE-Cadherin junctional accumulation; dotted lines outline the contour of LTp/GBs. (M1,M2) Imaris 3D reconstitution at two planes of LTp/GB cells labelled with nuclear and junctional markers, showing the transient pyramidal-like cell arrangement (in grey, the clipping tool of the Imaris software allowing cutting and following the 3D structure in different planes). Asterisks, position of the nucleus of the trailing (white) and leading (red) cells. (N) Schematic representation of cell arrangements during LTp/GB morphogenesis (leading cell in red and trailing cells in green; for simplification only the cell body of some trailing cells are depicted from stage 13 to 15). St, stage; e, early; m, middle; l, late.

(Fig. 1H). In particular, a group of six or seven cells were positioned around a common central ring encompassing their apical junctions (Fig. 1H,I,M). Subsequently, other cells were allocated into the branch and will connect the LTp/GB to the rest of the tracheal system; however, here we limit our analysis to this early and distal group of six or seven cells. At this stage, tip cells in the LTp/GBs could already be distinguished from the remaining cells of the bud, both by their more-elongated shape and higher protrusion activity (Fig. 1H,M, Fig. 2C). However, protrusion activity was not restricted to tip cells (Fig. 2C,E), but as the bud emerged from the placode, protrusion activity declined in all but one or a couple of cells at the leading front, similar to what occurs in late dorsal branches (Ribeiro et al., 2002; Caussinus et al., 2008) (Fig. 3A, see also Fig. 1B–D); trailing cells never completely ceased showing protrusion activity, as shown by individual cell labelling revealing that some of their filopodia ended up in a front position and could be wrongly attributed to tip cells (Fig. 2E). The bodies of tip cells became extremely flat, with a very long and growing lamellipodium-like structure harbouring many filopodia at its edges (Fig. 2C,D, see also Fig. 3A and Fig. 1C–E,J–L), an indication of leading cell morphology (Rørth, 2011). This is a specific and early feature of tip cells that is maintained throughout the subsequent extension of the branch (Fig. 2D, Fig. 3; supplementary material Movie 1). Indeed, individual cell tracing indicated that, unlike in other systems, such as in border cell migration (Bianco et al., 2007; Prasad and Montell, 2007), once cells acquired the morphological features of a tip cell, they remain as such during the LTp/GB morphogenesis and did not exchange this morphology and behaviour with the other cells of the branch in all the cases examined ($n>30$) (Fig. 3A,B; supplementary material Movie 1).

A transient ‘pyramidal’ arrangement reorganises LTp/GB cells into a longitudinal alignment

Tip and trailing cells in the bud were not all on the same plane and adopted a pyramid-like organisation, in which their apical surfaces cluster in a small circular area (Fig. 1M). This was a transient arrangement, as from stage 12 to 13, LTp/GB cells reorganised into a longitudinal alignment with their apical cell surfaces arranged in a row along a proximo-distal axis (Fig. 1H–L,N, Fig. 3B; supplementary material Fig. S1A–D,I–N). In a way, tracheal pyramids are reminiscent of rosettes in *Drosophila* germ

Journal of Cell Science (2014) 127, 465–474 doi:10.1242/jcs.142737

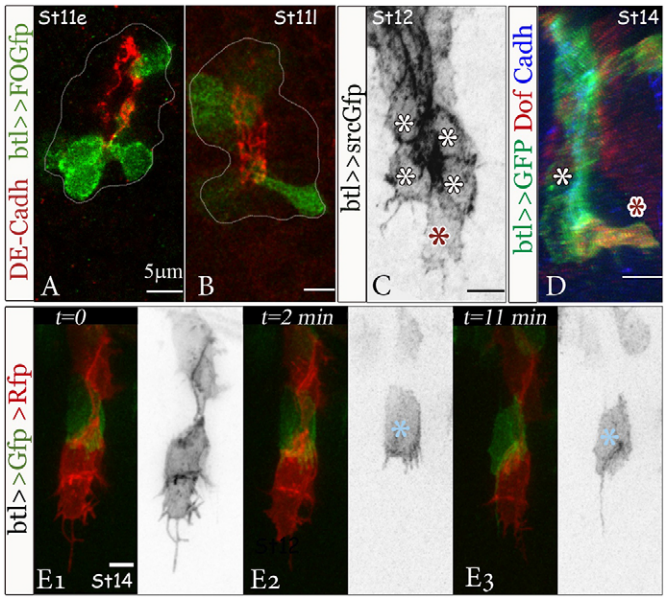

Fig. 2. Shape changes and protrusion activity of LTp/GB cells. (A,B) Individual cell labelling unveils cell shapes in LTp/GB morphogenesis at budding. (C) The tip cell (red asterisk) produces a big lamelipodia and filopodia, but trailing cells (white asterisks) do also have filopodia. (D) The protrusion from the tip cell changes its orientation at stage 14. (E1–E3) Snapshots from a live recording of a LTp/GB with distinct labelling of some cells with the brainbow system to clearly show filopodia from trailing cells [black and white images show the red (E1) and green (E2,E3) channels]. St, stage; e, early; l, late.

band extension, as both appear to be transient organisations suitable to drive cell rearrangements (Blankenship et al., 2006). However, unlike rosettes, tracheal pyramidal arrays include 'unequal' cells, namely tip and trailing cells; this is a crucial difference because tracheal cell rearrangement is precisely coupled to tip cell behaviour. In the *Drosophila* germ band, rosettes of similar cells act in rearranging cell clusters from being elongated along the embryonic dorsoventral axis to being elongated along the anteroposterior axis, without a significant difference in the type of cell cluster organisation (Zallen and Blankenship, 2008). Conversely, LTp/GB pyramids harbouring tip and trailing cells evolve into a new organisation of the cell cluster with increased anisotropy. It has been suggested that rosettes represent functional units of cell behaviour during tissue elongation (Blankenship et al., 2006); similarly, we would like to propose that pyramids act as functional units to allocate and organise clusters of cells into the LTp/GBs (Fig. 3B).

By stage 12, there was a change in the collective migration path of LTp/GB cell clusters; the two cells at the tip separated and behaved as independent leading cells (Fig. 3). As they approached two distinct groups of *bnl*-expressing cells, one cell moved towards a ventral group of *bnl*-positive cells and became the terminal cell, while the other moves posteriorly towards *bnl*-positive cells near the LTa (supplementary material Fig. S2H–J) and became the fusion cell connecting the LTp with the neighbouring LTa. Associated with the individual changes in the leading cells, the whole LTp/GB cell cluster reshaped following the alternative branching paths (Fig. 3A,B).

FGF signalling in the tip cells is sufficient to confer migratory capacity to the cell cluster

Can tip cells in the LTp/GB be defined on the basis of cytoskeleton features? Consistent with their morphology, tip cells showed strong actin accumulation at their basal membrane through all stages of branch morphogenesis (Fig. 4E,F, red arrows). In contrast, in trailing cells, and as cell protrusion declined, high actin accumulation was progressively restricted to their apical surface (Fig. 4E,F, white arrowhead and arrow, basal

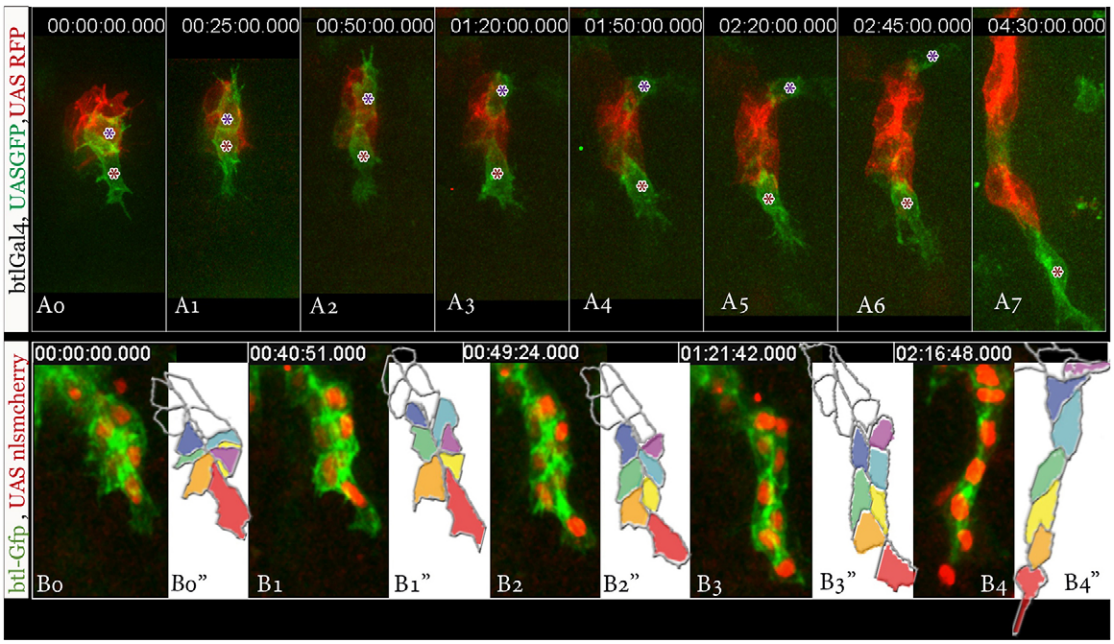

Fig. 3. Stereotypical pattern of cell movements during LTp/GB migration. (A0–A7) Snapshots from an *in vivo* recording of LTp/GB cells randomly expressing the GFP (green) or RFP (red) with the brainbow system (see Materials and Methods). Two tip cells (in green, asterisks) move in different directions and exchange neighbours. (B0–B4) Snapshots from an *in vivo* recording of LTp/GB cells labelled with nuclear (red) and cytoplasmic (green) markers and corresponding cartoons to show individual tracing of the whole cells. Time is hours:minutes:seconds:milliseconds.

Journal of Cell Science (2014) 127, 465–474 doi:10.1242/jcs.142737

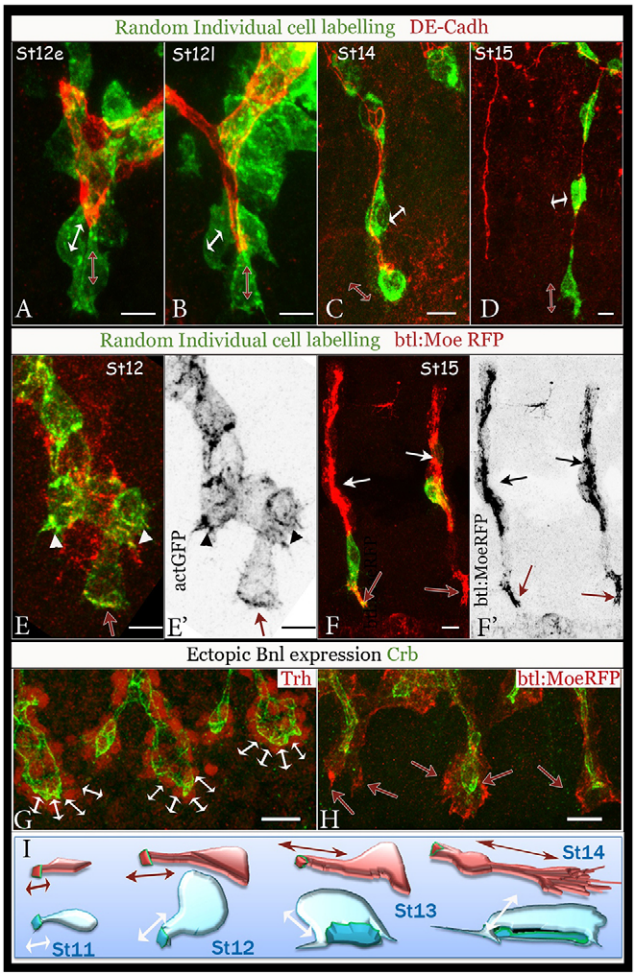

Fig. 4. Features of leading and trailing cells. (A–D) From stages 12 to 15, the apicobasal axis of LTp/GB trailing cells shifts from parallel to perpendicular to the direction of branch elongation (white double arrows) but remains parallel for the tip cells (red double arrows). Individual clones labelled by GFP flip-out clones. (E,F) Actin strongly accumulates basally in tip cells (red arrows), whereas there is a transition from strong basal (white arrowheads) to apical accumulation in trailing cells (white arrows), as detected by expression in group of cells of expressing either actGFP (green) at stage 12 (E) or btl-RFPMoe (red) at stage 15 (F). (G,H) *bnl* ectopic expression confers LTp/GB trailing cells features to tip cells in terms of apicobasal axis orientation (double arrows) and smaller apical surfaces as unveiled by Crb accumulation (green), and basal actin accumulation (by btl-RFPMoe, red in panel H; red arrows). Ectopic Bnl expression was driven by *insc*-Gal4 (G) and *en*-Gal4 (H). (I) Schematic representation of a leading (red) and a trailing (blue) cells according to the features at the different stages indicated. St, stage; e, early; l, late. Scale bars: 5 µm (A–F); 10 µm (G,H).

and apical actin, respectively). In addition, tip cells retained a constricted apical membrane, while trailing cells increased their apical surface (supplementary material Fig. S3A, Fig. S1). Furthermore, in trailing cells, the apical membrane was parallel to the direction of branch elongation (Fig. 4A–D,I, white arrows), while that of tip cells remained perpendicular to the direction of branch elongation (Fig. 4A–D,I, red arrows). Thus, three cytological features distinguish leading from trailing cells: a smaller apical surface, a proximo-distal orientation of their apicobasal axis, and actin accumulation at two prominent sites, one at the small apical junction and another at the basal membrane. Interestingly, all LTp/GB cells acquired these features upon ectopic expression of *bnl* (see Materials and Methods) (Fig. 4G,H), thus indicating that FGF signalling is responsible for the cytoskeletal organisation of leading cells.

Given that FGF signalling can induce the above-mentioned cytological features in any LTp/GB trailing cell, we would like to propose that all the effects of FGF signalling on LTp/GB tracheal morphogenesis could be accounted for by triggering leading cell fate and behaviour. It has been previously shown that, among the tracheal cells, those with higher levels of *btl* expression adopt the tip position (Ghabrial and Krasnow, 2006). However, in that experiment, genetic mosaic animals were generated in which some tracheal cells displayed higher *btl* levels than the others but all had some *btl* expression. Thus, we aimed to generate embryos with individual cells positive for the FGF receptor, while all the other tracheal cells would be completely deficient for the receptor. Remarkably, LTp/GB cells were observed to migrate and adopt their elongated morphology with just one FGF-receptor-positive cell at the tip position (Fig. 5C,D; for examples in other branches see supplementary material Fig. S2K). These results show that FGF signalling at the tip cells is sufficient to confer migratory capacity to the cluster and that the trailing cells follow the tip cells that act as leading cells. In all cases, FGF-receptor-positive cells accumulated at the tip positions. Interestingly, we found cases in which two FGF-receptor-positive cells occupied the position of the two tip cells, namely the future terminal cell and the future fusion cell, thus enabling the LTp/GB to migrate both towards the ventral midline and towards the neighbouring LTa (Fig. 5C,D).

The acquisition of leading cell features requires a shift between Rac activation and inactivation

It was previously suggested that Rac activation is an essential downstream event of tracheal cell motility induced by FGF signalling (Chihara et al., 2003). To examine whether there is a specific activation of Rac at the tip of the LTp/GB branch we used transgenic *Drosophila* expressing a fluorescence resonance energy transfer (FRET)-based sensor (Kardash et al., 2010), as previously used in cultured egg chambers (Wang et al., 2010). We worked to detect activity of this sensor *in vivo* in whole embryos (see Materials and Methods) and upon its expression with a tracheal driver we detected a distinct FRET signal at the tip positions of the LTp/GB, both at the ventral side and at the site of the future fusion with the neighbouring LTa (Fig. 5E,F; supplementary material Movie 2).

We then addressed the contribution of Rac activity in tip cells to LTp/GB migration. Given that embryos mutant for RhoGTPases do not allow the study of the specific tracheal roles of these proteins and because RNAi technology has a very limited effect at these stages of tracheal development, we turned to the analysis of the dominant-negative effect and constitutively activated forms of RhoGTPases (Ridley, 2001) under the control of a tracheal driver. First, and as previously described (Chihara et al., 2003), expression of constitutively active Rac (Rac^{ACT}) in all tracheal cells was found to induce the transformation described as an epithelial-to-mesenchymal transition; in particular, we observed the downregulation of junctional [E-Cadherin (DE-Cadh), α-Catenin (α-Cat)] and apical components, such as Crumbs (Crb) (Fig. 6E; supplementary material Fig. S2G5–7, Fig. S4G–I), associated with this transition (Chihara et al., 2003). Interestingly, analysis of Rac activity in individual cells by flip-out clones (see Materials and Methods) revealed that clones of dominant-negative Rac (Rac^{DN}) in otherwise wild-type LTp/GBs

Journal of Cell Science (2014) 127, 465–474 doi:10.1242/jcs.142737

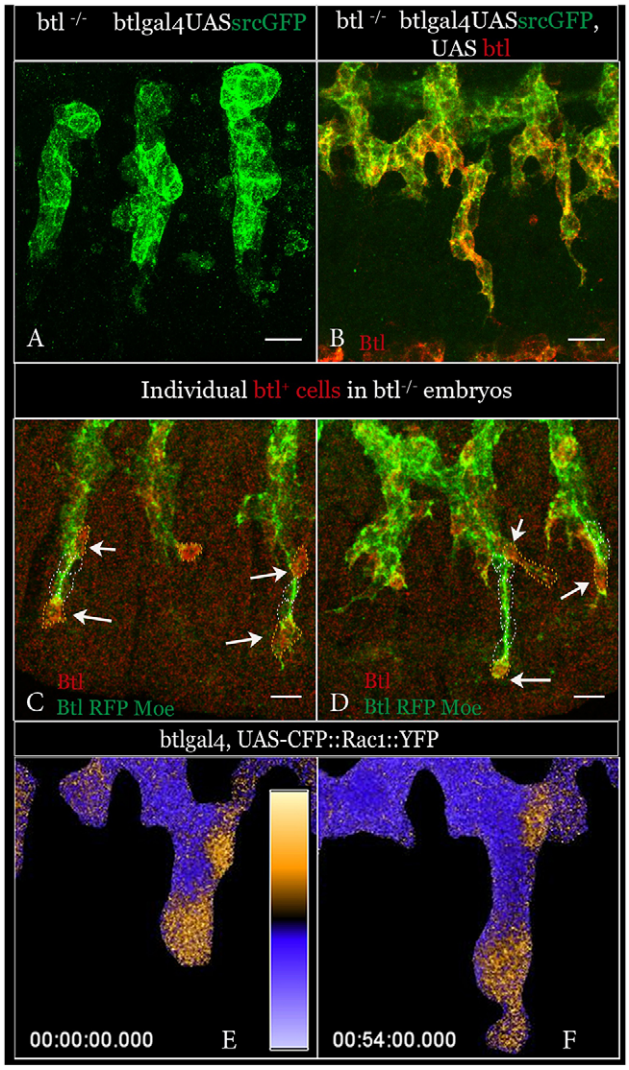

Fig. 5. FGF signalling in single cells can drive migration of LTp/GB cell clusters. (A) Tracheal cells fail to migrate in a *btl*-null mutant (btl^{LG19}) labelled with srcGFP. (B) Rescue of the btl^{LG19} phenotype by *btl* tracheal expression (this rescue is not always complete, probably owing to delayed expression with the Gal4/UAS system). (C,D) Examples of the rescue of the btl^{LG19} phenotype by *btl* expression in individual cells (in red); note that *btl*-positive cells accumulate at tip positions (arrows) and are associated with clusters of migratory cells (compare with A). btl^{+} flip-out clones are generated by heat shock (see Materials and Methods). (E,F) Snapshots from an *in vivo* recording of an LTp/GB from an embryo bearing a (FRET)-based sensor with a distinct signal at the leading cell positions, both at the ventral side and at the site of the future branch fusion. Time is hours:minutes:seconds:milliseconds. Scale bars: 10 µm.

are almost never associated with tip cells and correspond to trailing cells (Fig. 6K; supplementary material Fig. S3B), consistent with the above-mentioned suggestion that Rac activation is an essential event downstream of FGF-induced tracheal cell motility. However, and more surprisingly, clones of Rac^{ACT} in otherwise wild-type LTp/GBs were also not associated with tip cells, and the few clones in the branch corresponded to trailing cells (Fig. 6L; supplementary material Fig. S3B). These observations indicate not only a strict requirement of Rac activity for the acquisition of leading cell features but also the need for a temporal shift between Rac activation and inactivation and/or an asymmetric intracellular display of Rac activity.

Individual cell labelling reveals connections between distant cells in the LTp/GB cluster

The experiments reported so far address the specification and features of tip cells; in particular they show that restricting FGF signalling to tip cells is sufficient to provide migratory capacity to whole clusters. We next addressed the trailing cell features in the cluster migration. Once the cell clusters exit the pyramid arrangement and adopt a longitudinal organisation, the LTp/GBs also grow by cell intercalation, as cells evolve from a side-by-side to an end-to-end cell arrangement and exchange intercellular adherens junctions with autocellular ones (Ribeiro et al., 2004). Unexpectedly, cells were found to be in contact not only with neighbouring ones, but also with distant ones through long extensions, as appreciated by live imaging (Fig. 6A,B). Indeed, *in vivo* recording of the said cells showed that they had previously been close but had subsequently exchanged neighbours. Connections with distant cells are established by cytoplasmic extensions that are often longer than one cell body [11.8 µm±1.3 (s.d.)] and that accumulate actin (Fig. 6B), but not DE-Cadh or Crb (data not shown).

Modification of LTp/GB cell properties by dominant-negative and constitutively active Rho mutants

In order to analyse how cell features affect cluster migration following the FGF-induced changes in the leading cells, we resorted to the study of the mutant phenotypes for the RhoGTPases Cdc42 and Rho, which are key cytoskeleton regulators (Hall, 2005; Jaffe and Hall, 2005), as previously performed for the RhoGTPase Rac (Chihara et al., 2003). A unidirectional assignment between a specific cellular process *in vivo* and a single RhoGTPase is probably an oversimplification as each RhoGTPase might be simultaneously involved in more than one process in the same cell (Pertz, 2010). However, the modification of cell properties by RhoGTPases mutant forms, although not a direct effect, has proven very useful as it allows us to modify cell features, which cannot be achieved by modulation of a single of their downstream effectors.

A dominant-negative form of Rho (Rho^{DN}) produced breaks and detachment of LTp/GB cells (Fig. 6F, asterisks), which then migrated in small groups (in 48% of branches) or individually (in 23% of branches) (supplementary material Fig. S3C,D). In Rho^{DN} cells, DE-Cadh and other apical proteins adopted a fragmented distribution (Fig. 6F′; supplementary material Fig. S2B5–7, Fig. S4J–L), suggesting impaired cell adhesion, which could account for this phenotype. Consistently, upon expression of constitutively active Rho (Rho^{ACT}), we observed that LTp/GB cells held together, from the early stages, in a pyramidal-like configuration and showed impaired migration (more than 50% of branches not elongating) (Fig. 6G; supplementary material Fig. S3C, Fig. S2C, Fig. S4M–O). Reinforcing the notion of increased cell adhesion as a cause of the Rho^{ACT} phenotype, we observed that a decrease in adherens junction components significantly ameliorated the phenotype (see Materials and Methods; supplementary material Fig. S3E). Conversely, impairment of migration in Rho^{ACT} cells did not appear to depend on decreased cell motility, as cells remained protrusive (supplementary material Fig. S2C1–4). In particular, tip cells emitted very long projections and adopted a highly elongated shape (Fig. 6G, red arrows) and, although they failed to migrate, they still responded to chemoattractant signals, thus indicating that migration and response to chemoattractant are two separable processes. Expression of either Rho^{ACT} or Rho^{DN} in clones reproduced the

Journal of Cell Science (2014) 127, 465–474 doi:10.1242/jcs.142737

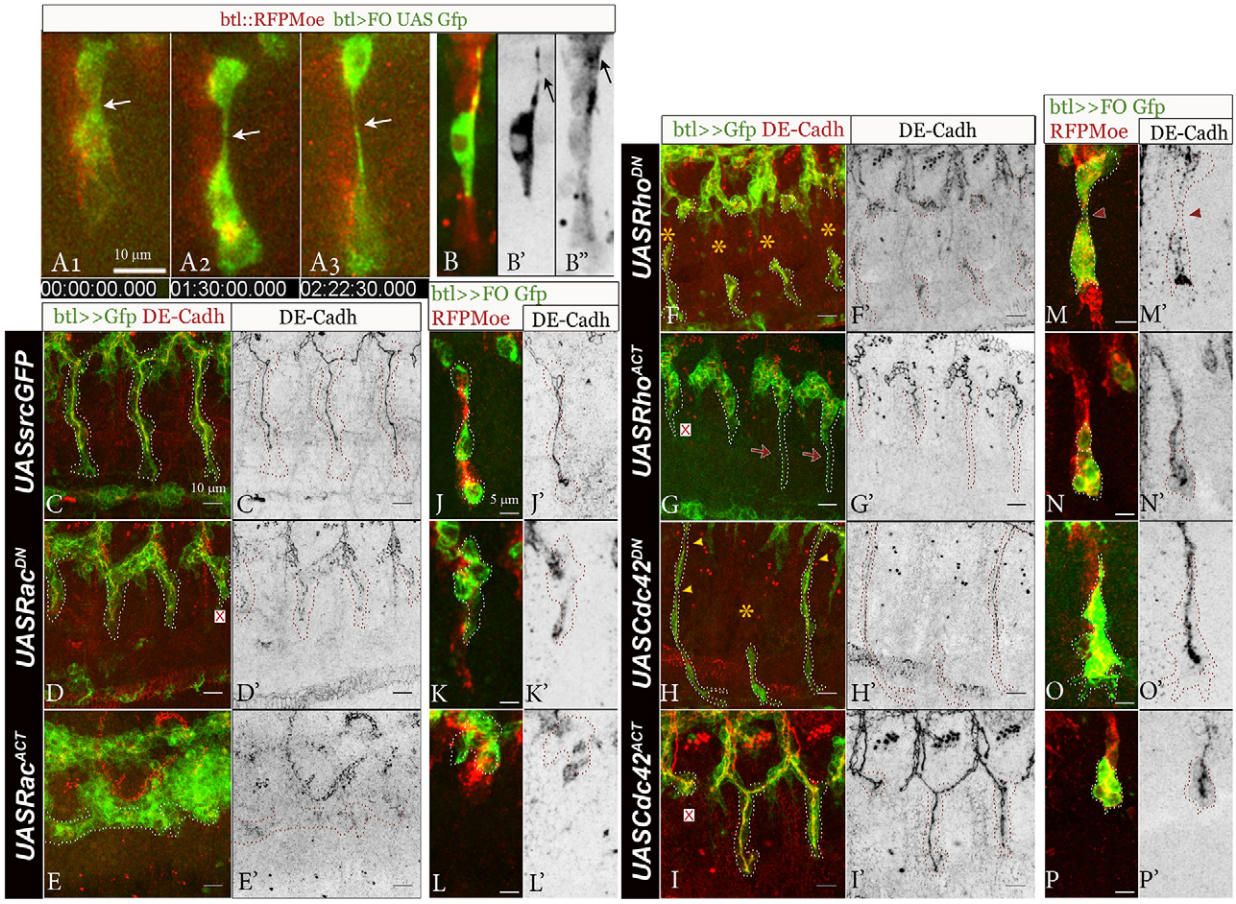

Fig. 6. Modification of cell features by mutant forms of the Rho GTPases. (A1–A3) *In vivo* recordings show long cytoplasmic extensions between close cells that get apart. Time is hours:minutes:seconds:milliseconds. (B) Individual cell labelling *in vivo* shows that these extensions have actin accumulation. (B′,B″) The same panels as B, to show the shape of individual cells (B′) and actin (btl-RFPMoe) accumulation (B″). (C–I) Phenotypes upon tracheal expression of constitutively active and dominant negative forms of Rac, Rho and Cdc42. Most of the LTp/GBs do not elongate upon Rho and Cdc42 constitutive activity (red crosses) and Rho and Cdc42 inactivation causes breaks (asterisks). (C′–I′) The same panels as C–I to show DE-Cadh junctional accumulation. (J–P) Phenotypes associated with expression of mutant RhoGTPases in individual cells (in green) in otherwise wild-type LTp/GBs (wild-type cells in red); (J′–P′) same panels to show DE-Cadh junctional accumulation. FO, flip-out. Scale bars: 10 µm (A,C–I); 5 µm (J–P).

main features of the respective phenotypes even when expressed in few cells (Fig. 6N,M); thus, for example, we observed that just a few Rho^{DN} cells detached from the branch (Fig. 6M). Interestingly, however, Rho^{ACT} single cell clones at the tip of normally elongated LTp/GBs did not show the long extensions observed when the whole branches were mutant (compare Fig. 6N and Fig. 6G). This finding reinforces the interpretation that these extensions are not a cell-autonomous effect of the constitutive activity of Rho but of the incapacity of the cells to migrate, even though they could respond to the chemoattractant signals.

Modification of LTp/GB cell properties by Cdc42 dominant negative and constitutively active mutants

Upon tracheal expression of a dominant-negative form of Cdc42 ($Cdc42^{DN}$), LTp/GB, cells were associated by thin extensions, as if they were overstretched (68% of elongating branches with overstretching) (Fig. 6H, arrowheads; supplementary material Fig. S3C), with discontinuous accumulation of either DE-Cadh, α-Cat or Crb, found even in the main cell body (Fig. 6H′; supplementary material Fig. S2D5–7, Fig. S4P–R). Moreover, *in vivo* recordings suggested that overstretching caused some breaks in $Cdc42^{DN}$ cells. However, breaks were fewer than with Rho^{DN} (small groups of migrating cells detached from 7% of the branches and individual migration of leading cells occurred in 17% of the branches) (supplementary material Fig. S3D). The differences in the breaks between Rho^{DN} and $Cdc42^{DN}$ cells did not appear to depend on variations in the strength of the transformations associated with each construct. Instead, other features of the phenotype suggested that the overstretching, and thus the breaks in $Cdc42^{DN}$, was due to increased motility. Thus, for example, trailing cells in $Cdc42^{DN}$ mutants showed more protrusions and were more actin-enriched basally than wild-type cells (supplementary material Fig. S2D1–4), features normally associated with leading cells. Accordingly, we detected many cases in which trailing cells, while still attached to the cluster, appeared to initiate a new migratory path (in 28% of branches) (supplementary material Fig. S3D). Moreover, *in vivo* recording showed some trailing cells taking the lead of the migratory cluster replacing the previous leading cell – a feature never observed in wild-type clusters – with eventually one or both cells detaching and migrating individually (supplementary material Movie 3). In addition, and unlike in the wild-type, distal trailing cells also exchanged positions inside the cluster with more proximal

Journal of Cell Science (2014) 127, 465–474 doi:10.1242/jcs.142737

trailing cells (supplementary material Movie 3). Consistent with higher motility in Cdc42^{DN} cells, expression of constitutively activate Cdc42 (Cdc42^{ACT}) reduced the motility of LTp/GB cells, as the transient pyramidal organisation did not evolve, or evolved much more slowly, towards branch elongation (Fig. 6I; supplementary material Fig. S3E5–7, Fig. S4S–U), causing more than 50% of branches not to elongate (supplementary material Fig. S3C). In addition, and reinforcing the interpretation of decreased motility in Cdc42^{ACT}, cells looked smooth and non-protruding (supplementary material Fig. S2E1–4), in contrast to the appearance of cells in Rho^{ACT} (supplementary material Fig. S2C1–4). The corresponding phenotypes were also observed upon expression in clones of each mutated form. Cdc42^{ACT} cells did not move apart; in some cases they did not get even allocated into different branches, and, if at the tip, they were sometimes associated with lack of branch elongation (Fig. 6P). Cdc42^{DN} cells displayed extensions, although with no breaks (Fig. 6O).

Rho and Cdc42 dominant-negative and constitutively active mutants modify the migration speed of the LTp/GB

Analysis of kymographs depicting the positions of cells over time allowed us to study how the above-mentioned cell changes impinge on migration of the LTp/GB clusters (example of wild-type versus Cdc42^{DN} in Fig. 7A,B). We found a strong reduction in the migration speed, as measured by the distance reached by the leading cell, in the case of Rho^{CA} (2.5±2.3 nm/second, n=3) and Cdc42^{CA} mutants (2.8±0.64 nm/second, n=8) compared to the wild-type (4.5±0.66 nm/second, n=19). Conversely, speed increased in Rho^{DN} (5.4±1 nm/second, n=36) and Cdc42^{DN} mutants (7.2±1.75 nm/second, n=37), a rise that was higher when mutant conditions were associated with branch breaks (8.5±1.8 nm/second, n=11 for Rho^{DN} and 9.8±2.5 nm/second n=10 for Cdc42^{DN}) than when branches kept their integrity (4±0.67 nm/second n=20 for Rho^{DN} and 5.4±2 nm/second n=21 for Cdc42^{DN}), the latter being consistent with the observations from laser-induced cuts in wild-type branches (Caussinus et al., 2008). Thus, mutant conditions with lower migratory speeds matched compact LTp/GBs whereas those with higher migratory speeds matched overstretched and/or broken LTp/GBs.

Effect of constitutive activity of Rho in a *btl* mutant background

Given that we detect an effect of Rho and Cdc42 mutant forms in trailing cells, Rho and Cdc42 appear to modify tracheal cell properties in the LTp/GB cluster in an FGF-independent manner. To confirm this hypothesis we examined the effect of Rho^{ACT} tracheal expression in a mutant background for *btl*, the gene encoding the FGFR in the trachea. Under these circumstances, tracheal cells were more tightly packed than in just *btl* mutants. This observation supports the notion that Rho activity increases cell adhesion in a way that is independent of the FGF signalling triggering migration (supplementary material Fig. S3F).

DISCUSSION

FGF and collective migration

As pointed out in the Introduction, the FGF signalling pathway is involved in many morphogenetic events requiring collective migration of cell clusters. However, it is not entirely clear whether in these events FGF signalling is directly involved in triggering cell migration, or alternatively if it is required for other processes such as cell determination that only affect cell migration indirectly. Moreover, although FGF might be

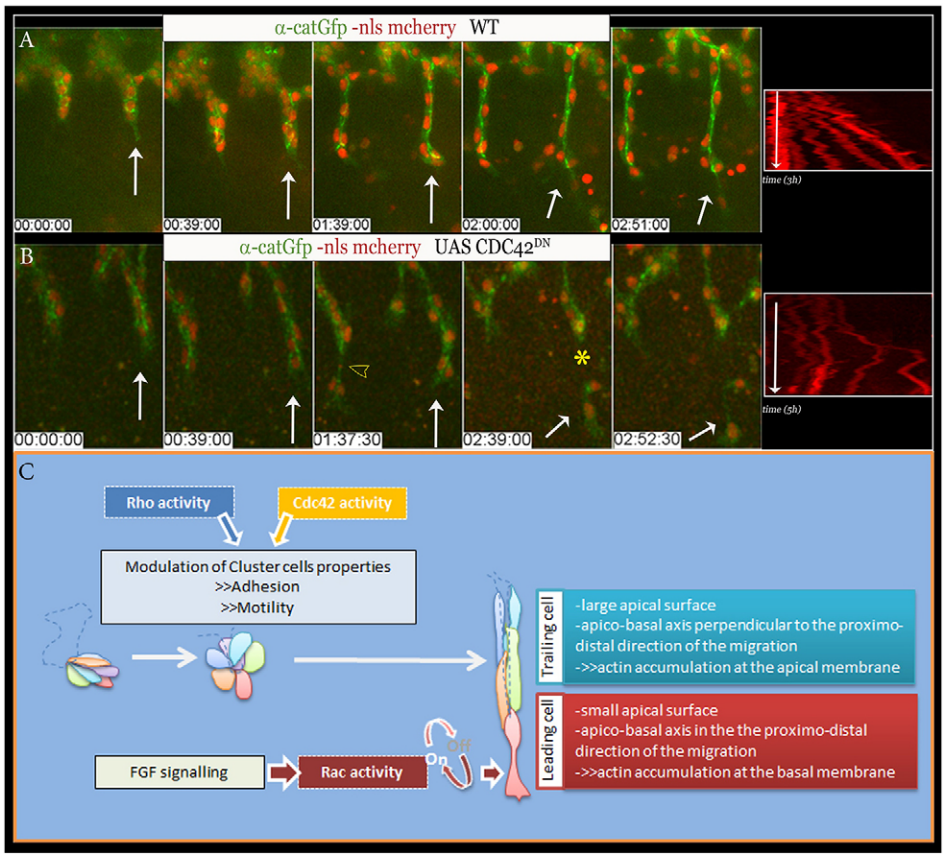

Fig. 7. Migratory behaviour of wild-type and mutant LTp/GBs and model for their cell specification. (A,B) Snapshots from *in vivo* recordings of LTp/GBs from a wild-type embryo (A) and from an embryo upon tracheal expression of a dominant-negative form of Cdc42 (B); red, a nuclear marker; green, α-Cat–GFP. Arrowhead, detachment of cells; yellow asterisk, branch break recorded in the kymograph. The corresponding kymograph of each metamere (indicated by the white arrow) is shown in the right panel, each line indicating the position of each nucleus at different times, thus allowing an evaluation of their displacement. Time is hours:minutes:seconds. (C) A model for the specification of leading and trailing cells in LTp/GB morphogenesis.

Journal of Cell Science (2014) 127, 465–474 doi:10.1242/jcs.142737

required, it is not clear either whether all the cells or just a subset of those need to directly receive the signal to sustain the migration of the entire cluster. One well-studied case is the role of FGF in the development of the zebrafish lateral line. In that case, FGF appears to be produced by the leading cells, which signal to the trailing cells, the cells where FGF signalling is active. Restriction of FGF signalling is thereafter required for the asymmetric expression of the receptors for the chemokines that guide migration (Aman and Piotrowski, 2008).

A very different scenario applies in the case of *Drosophila* tracheal migration. On the one hand, FGF is expressed in groups of cells outside the migrating cluster (Sutherland et al., 1996). On the other hand, our results in the LTp/GB indicate that FGF signalling is required and sufficient in the leading cells, and not in the trailing cells, for the migration of the whole cell cluster. Therefore, in spite of its widespread involvement, the mechanisms triggered by FGF signalling in collective migration appear to be quite different.

Rho, Cdc42, adhesion and motility

The above-described experiments revealed that Rho inactivation produced breaks and detachment in the LTp/GB cluster, whereas its constitutive activation let these cells to hold together, impairing migration. Likewise, upon Cdc42 inactivation LTp/GB cells had thin extensions that were associated, in some cases, with breaks, whereas upon its constitutive activation, the LTp/GB transient pyramidal organisation did not evolve, or evolved much more slowly, towards branch elongation. However, the phenotypes from each of the RhoGTPase mutants are not alike and our detailed analysis suggests that Rho impinges primarily on cell adhesion whereas Cdc42 does so on cell motility.

These results are consistent with previous findings that show a role for Rho in regulating adherens junction stability (Braga et al., 1997; Bloor and Kiehart, 2002; Magie et al., 2002) and for Cdc42 as the main mediator of filopodia formation (Nobes and Hall, 1995; Ridley, 2006; Pedersen and Brakebusch, 2012). We note, however, that we have found Cdc42 to exert in the LTp/GB an opposite effect to the one identified in other systems, that is, $Cdc42^{DN}$ mutants showed more protrusions and were more actin-enriched basally than wild-type cells and $Cdc42^{ACT}$ mutants showed a reduced motility.

There is an increasing amount of data pointing to the different effect of RhoGTPases *in vitro* versus *in vivo* models and also among various cell types (Pedersen and Brakebusch, 2012). As mentioned before, a unidirectional assignment between a specific cellular process *in vivo* and a single RhoGTPase is probably an oversimplification and this was not the aim of our study. Rather we relied on mutant forms of the RhoGTPases to modulate cell features, either individually or collectively, to assess their role in the overall behaviour of the cell cluster. In doing so, our results point to a crucial role for a balance between cell adhesion and cell motility for the collective migration of a cell cluster (see below).

A model for the collective migration of LTP/GB cells

Our results support the following model for the specification, features and behaviour of leading cells in the migration of the LTp/GB branch (Fig. 7C). Upon signalling from the FGF pathway, tip cells reorganise their cytoskeleton features (actin enrichment at the basal membrane, small apical surface and an apicobasal polarity along the proximo-distal axis), thereby enabling them to acquire leading behaviour. Indeed, FGF can induce migratory capacity to the whole cluster by signalling only to the tip cells, where a dynamic transition between states of Rac activity is needed to acquire a leading role. How the behaviour of tip cells leads collective migration thereafter depends on the features of the cells in the cluster, which are determined by various different regulators, among these, the RhoGTPases, which act, at least in part, in an FGF-independent manner. Ultimately, the balance between individual cell properties, such as cell adhesion, motility and apicobasal polarity will (1) determine the net movement of the overall cell bodies or alternatively changes in cell shape in terms of elongation, (2) control the migratory speed, and (3) define whether cells will migrate individually or in clusters and whether clusters will bifurcate in different paths. The combined effect of the changes promoting leading cell behaviour and modulation of cell features is likely to be a widely exploited mechanism in collective migration. In particular, the actual balance between these cell features might dictate the specifics of each migratory process and, consequently, the final shape of the tissues and organs they contribute to generate.

MATERIALS AND METHODS

Drosophila stocks and genetics

Details for all genotypes and transgenes can be found in flybase (http://flybase.org) or in the references listed here. Unless otherwise noted, stocks were obtained from the Bloomington Stock Center. The Gal4/UAS system (Brand and Perrimon, 1993) was used to overexpress or misexpress proteins. Unless otherwise noted, transgenes were driven by the pantracheal driver *btl*Gal4 (Shiga et al., 1996) recombined with either srcGFP, catGFP or GMAGFP. In supplementary material Fig. S2 and Fig. S4 we used it in combination with the btlmoeGFP construct (from Markus Affolter, Basel University, Switzerland). For expression in groups or individual tracheal cells we used, (1) the FLP-out technique (Fig. 2A, Fig. 4A–F, Fig. 6A,B,J–P; supplementary material Fig. S2K, Fig. S3B) with the hsFlp122; *btl*RFPMoe, *btl* $>y^{+}>$Gal4 stock (Ribeiro et al., 2004) combined with the UAS constructs for the diverse RhoGTPase variants and/or UAS-srcGFP, and (2) the brainbow system (Fig. 2B,E, Fig. 3A; supplementary material Movie 1) with the hsCre; *btl*Gal4, UAS-Brainbow stock (Förster and Luschnig, 2012). For the *btl* rescue experiments and for *Rho1* expression in *btl* mutants we generated the following stocks: (1) btlGal4UASsrcGFP;btl^{LG19}, (2) UAS btl; btl^{LG19}, (3) UAS btl, UASsrcGFP; btl^{LG19}, (4) hsFlp122; *btl*RFPMoe, *btl* $>y^{+}>$Gal4,btl^{LG19}, and (4) UAS Rho^{ACT}, btl^{LG19}. Misexpression of *bnl* (UAS-*bnl*) was induced using either *insc*Gal4 (Fig. 4G) or *en*Gal4*src*GFP (Fig. 4H). Flies bearing the Rac construct for FRET are as reported previously (Wang et al., 2010). Genotypes were identified by absence of β-galactosidase expression from 'blue' balancers. All crosses and staging were performed at 25°C. For the FLP-out experiments, embryos were heat shocked for 45 minutes at 37°C and transferred at room temperature for 6 hours before mounting. Wild-type and mutant LTp/GBs were scored from the central region of embryos (the five metameres 4–8) to ensure the comparison of between branches with similar development. To reduce α-Cat levels in genetic interaction experiments we used *cat* RNAi lines from Bloomington. The total number (*n*) of embryos and/or branches is given in the text and legends where appropriate. Data are means±s.e.m.

Immunostaining, whole mount *in situ* and image acquisition

Embryos were staged as in Campos-Ortega and Hartenstein (Campos-Ortega and Hartenstein, 1985) and stained following standard protocols. A *bnl* RNA probe was generated from a cDNA corresponding to amino acids 241–400. Whole mount *in situ* followed by immunostaining was performed according to standard protocols. The following primary antibodies were used: rabbit anti-β-galactosidase (Cappel) (1:300); goat anti-GFP (1:600) and rabbit anti-RFP (1:300) (Abcam); mouse anti-DE-Cadh (1:100) (DCAD2-DSHB); anti-Crb (1:10) (Cq4-DSHB); mouse anti-Dlg (1:500); rabbit anti-DaPKC (1:500), rabbit anti-SAS (1:250); rat

anti-Trh (1:600) and rat anti-Btl (1:10) (N. Martín in our laboratory); and rabbit anti-Dof (1:250) (gift from Jayan Nair and Maria Leptin, EMBL, Heidelberg, Germany). Embryos were fixed in 4% formaldehyde for 20–30 minutes and for 10 minutes for DE-Cadh. Immunostaining was detected with donkey secondary antibodies labelled with Alexa Fluor 488, Alexa Fluor 555 or Alexa Fluor 649 (Invitrogen). Fluorescent images were obtained by using confocal microscopy (Leica TCS-SP5-AOBS system, Leica TCS-SPE microscope). Images are maximum projections of confocal *z*-sections unless otherwise noted. Images were post-processed with Fiji and assembled into figures using both Fiji and the Adobe Photoshop software.

FRET analysis

FRET images of live embryos were acquired with a Leica Sp5 confocal microscope equipped with HyD detectors, providing very low background levels. A 458 nm laser was used to excite the sample. CFP and YFP emission signals were collected simultaneously through channel I (470–510 nm) and channel II (525–600 nm), respectively. To capture images, a 63× 1.4 NA oil immersion objective was used with a zoom of 2 to 3. CFP and YFP images were processed with the Fiji bundle of ImageJ (Wayne Rasband, NIH). Gaussian Blur (sigma=2) filtering was applied to both channels prior to calculations. The YFP image was thresholded and converted into a binary mask with background set to zero and covering only the region of interest. This mask was applied to each channel and the resulting images were used to, in this sequence: (1) normalise intensity in time to correct for photobleaching and/or fluorescence expression increase, (2) equalise intensities (multiplication factor) to obtain identical average across the whole image, (3) obtain the FRET ratio by dividing the YFP by the CFP images, thereby leading to a histogram distribution centred on 1 (thanks to the equalisation). A specific look-up table ('ICA' in Fiji) was employed to visualise FRET ratios <1 in blue and >1 in yellow, histograms limits were set from 0 to 2, and FRET ratios near 1 appeared black, see Fig. 5E,F and supplementary material Movie 2. The local differences in FRET ratios were thereby visualised within the branch and a specific tip-enhancement was clearly observed in four recordings.

Time-lapse experiments, image processing and kymograph analysis

Embryos were mounted as described previously (Caussinus et al., 2008). Images were collected on a Leica TCS-SP5-AOBS system (Fig. 5E,F, Fig. 6B; supplementary material Movies 2, 3) or in an Andor Revolution spinning disk confocal (Fig. 2E, Fig. 3, Fig. 6A, Fig. 7; supplementary material Fig. S2, Movie 1). Sections were recorded every 100 seconds (Fig. 3A; supplementary material Movie 1), 60 seconds (Fig. 3B, Fig. 5E,F; supplementary material Movie 2), 90 seconds (Fig. 7A; supplementary material Fig. S3, Movie 3), and 150 seconds (Fig. 7B). *z*-stacks were collected with optical sections at maximum 1-µm intervals, and only LTp/GBs metameres from fourth to eighth were analysed. Image processing was performed with Fiji (http://fiji.sc/wiki/index.php/Fiji) and custom programming scripts in Fiji. The *z*-stacks projections were corrected in *x* and *y* dimensions by manual registration using a reference point tracking. Fig. 5 and data on the velocity of the tip cell were generated with a custom kymograph macro in Fiji. The number of metameres analysed for each condition were: wild-type, 19, Rho^{DN}, 36; $Cdc42^{DN}$, 37; Rac^{DN}, 16; Rho^{ACT}, 3; and $Cdc42^{ACT}$, 8.

Acknowledgements

We thank M. Affolter, S. Luschnig, X. Wang, the Bloomington Stock Center and Imaris Bitplane for fly stocks, reagents and software; N. Martin and E. Butí for help with *in situ* hybridisation and E. Fuentes and Y. Ribera for technical assistance; colleagues in the laboratory and X. Franch-Marro, S. Tosi and J. Colombelli for discussions; S. Araujo, M. Averof, K. Campbell, X. Franch-Marro, M. Furriols, M. Llimargas and M. Strigini for comments on the manuscript; and L. Bardia, A. Lladó and J. Colombelli for assistance with microscopy.

Competing interests

The authors declare no competing interests.

Author contributions

G.L. and J.C. designed the experiments, G.L. performed the experiments, G.L. and J.C. discussed the results, and J.C. wrote the manuscript.

Funding

This work has been supported by the Generalitat de Catalunya, the Spanish Ministerio de Ciencia e Innovacion and its Consolider-Ingenio 2010 program. G.L. was supported by Fondation pour la Recherche Médicale [grant number SPE20081214952]; the European Molecular Biology Organisation [grant number ALTF 978-2009] and Consejo Superior de Investigaciones Científicas.

Supplementary material

Supplementary material available online at
http://jcs.biologists.org/lookup/suppl/doi:10.1242/jcs.142737/-/DC1

References

Aman, A. and Piotrowski, T. (2008). Wnt/beta-catenin and Fgf signaling control collective cell migration by restricting chemokine receptor expression. *Dev. Cell* **15**, 749-761.

Bae, Y. K., Trisnadi, N., Kadam, S. and Stathopoulos, A. (2012). The role of FGF signaling in guiding coordinate movement of cell groups: guidance cue and cell adhesion regulator? *Cell Adh. Migr.* **6**, 397-403.

Bianco, A., Poukkula, M., Cliffe, A., Mathieu, J., Luque, C. M., Fulga, T. A. and Rørth, P. (2007). Two distinct modes of guidance signalling during collective migration of border cells. *Nature* **448**, 362-365.

Blankenship, J. T., Backovic, S. T., Sanny, J. S., Weitz, O. and Zallen, J. A. (2006). Multicellular rosette formation links planar cell polarity to tissue morphogenesis. *Dev. Cell* **11**, 459-470.

Bloor, J. W. and Kiehart, D. P. (2002). Drosophila RhoA regulates the cytoskeleton and cell-cell adhesion in the developing epidermis. *Development* **129**, 3173-3183.

Braga, V. M., Machesky, L. M., Hall, A. and Hotchin, N. A. (1997). The small GTPases Rho and Rac are required for the establishment of cadherin-dependent cell-cell contacts. *J. Cell Biol.* **137**, 1421-1431.

Brand, A. H. and Perrimon, N. (1993). Targeted gene expression as a means of altering cell fates and generating dominant phenotypes. *Development* **118**, 401-415.

Campos-Ortega, A. J. and Hartenstein, V. (1985). *The Embryonic Development of Drosophila melanogaster.* pp. 10-84. Springer-Verlag, New York.

Caussinus, E., Colombelli, J. and Affolter, M. (2008). Tip-cell migration controls stalk-cell intercalation during Drosophila tracheal tube elongation. *Curr. Biol.* **18**, 1727-1734.

Chihara, T., Kato, K., Taniguchi, M., Ng, J. and Hayashi, S. (2003). Rac promotes epithelial cell rearrangement during tracheal tubulogenesis in Drosophila. *Development* **130**, 1419-1428.

Ciruna, B. and Rossant, J. (2001). FGF signaling regulates mesoderm cell fate specification and morphogenetic movement at the primitive streak. *Dev. Cell* **1**, 37-49.

Förster, D. and Luschnig, S. (2012). Src42A-dependent polarized cell shape changes mediate epithelial tube elongation in Drosophila. *Nat. Cell Biol.* **14**, 526-534.

Friedl, P. and Gilmour, D. (2009). Collective cell migration in morphogenesis, regeneration and cancer. *Nat. Rev. Mol. Cell Biol.* **10**, 445-457.

Ghabrial, A. S. and Krasnow, M. A. (2006). Social interactions among epithelial cells during tracheal branching morphogenesis. *Nature* **441**, 746-749.

Ghabrial, A., Luschnig, S., Metzstein, M. M. and Krasnow, M. A. (2003). Branching morphogenesis of the Drosophila tracheal system. *Annu. Rev. Cell Dev. Biol.* **19**, 623-647.

Griffin, K., Patient, R. and Holder, N. (1995). Analysis of FGF function in normal and no tail zebrafish embryos reveals separate mechanisms for formation of the trunk and the tail. *Development* **121**, 2983-2994.

Hall, A. (2005). Rho GTPases and the control of cell behaviour. *Biochem. Soc. Trans.* **33**, 891-895.

Jaffe, A. B. and Hall, A. (2005). Rho GTPases: biochemistry and biology. *Annu. Rev. Cell Dev. Biol.* **21**, 247-269.

Kardash, E., Reichman-Fried, M., Maître, J. L., Boldajipour, B., Papusheva, E., Messerschmidt, E. M., Heisenberg, C. P. and Raz, E. (2010). A role for Rho GTPases and cell–cell adhesion in single-cell motility in vivo. *Nat. Cell Biol.* **12**, 47-53.

Lecaudey, V., Cakan-Akdogan, G., Norton, W. H. and Gilmour, D. (2008). Dynamic Fgf signaling couples morphogenesis and migration in the zebrafish lateral line primordium. *Development* **135**, 2695-2705.

Magie, C. R., Pinto-Santini, D. and Parkhurst, S. M. (2002). Rho1 interacts with p120ctn and alpha-catenin, and regulates cadherin-based adherens junction components in Drosophila. *Development* **129**, 3771-3782.

Nobes, C. D. and Hall, A. (1995). Rho, rac, and cdc42 GTPases regulate the assembly of multimolecular focal complexes associated with actin stress fibers, lamellipodia, and filopodia. *Cell* **81**, 53-62.

Pedersen, E. and Brakebusch, C. (2012). Rho GTPase function in development: how in vivo models change our view. *Exp. Cell Res.* **318**, 1779-1787.

Pertz, O. (2010). Spatio-temporal Rho GTPase signaling - where are we now? *J. Cell Sci.* **123**, 1841-1850.

Prasad, M. and Montell, D. J. (2007). Cellular and molecular mechanisms of border cell migration analyzed using time-lapse live-cell imaging. *Dev. Cell* **12**, 997-1005.

Journal of Cell Science (2014) 127, 465–474 doi:10.1242/jcs.142737

Ribeiro, C., Ebner, A. and Affolter, M. (2002). In vivo imaging reveals different cellular functions for FGF and Dpp signaling in tracheal branching morphogenesis. *Dev. Cell* **2**, 677-683.
Ribeiro, C., Neumann, M. and Affolter, M. (2004). Genetic control of cell intercalation during tracheal morphogenesis in Drosophila. *Curr. Biol.* **14**, 2197-2207.
Ridley, A. J. (2001). Rho GTPases and cell migration. *J. Cell Sci.* **114**, 2713-2722.
Ridley, A. J. (2006). Rho GTPases and actin dynamics in membrane protrusions and vesicle trafficking. *Trends Cell Biol.* **16**, 522-529.
Rørth, P. (2011). Whence directionality: guidance mechanisms in solitary and collective cell migration. *Dev. Cell* **20**, 9-18.
Rørth, P. (2012). Fellow travellers: emergent properties of collective cell migration. *EMBO Rep.* **13**, 984-991.
Samakovlis, C., Hacohen, N., Manning, G., Sutherland, D. C., Guillemin, K. and Krasnow, M. A. (1996). Development of the Drosophila tracheal system occurs by a series of morphologically distinct but genetically coupled branching events. *Development* **122**, 1395-1407.
Shiga, Y., Tanaka-Matakatsu, M. and Hayashi, S. (1996). A nuclear GFP/β-galactosidase fusion protein as a marker for morphogenesis in living Drosophila. *Dev. Growth Differ.* **38**, 99-106.
Sutherland, D., Samakovlis, C. and Krasnow, M. A. (1996). branchless encodes a Drosophila FGF homolog that controls tracheal cell migration and the pattern of branching. *Cell* **87**, 1091-1101.
Wang, X., He, L., Wu, Y. I., Hahn, K. M. and Montell, D. J. (2010). Light-mediated activation reveals a key role for Rac in collective guidance of cell movement in vivo. *Nat. Cell Biol.* **12**, 591-597.
Zallen, J. A. and Blankenship, J. T. (2008). Multicellular dynamics during epithelial elongation. *Semin. Cell Dev. Biol.* **19**, 263-270.